Analytical Methods

Accepted Manuscript

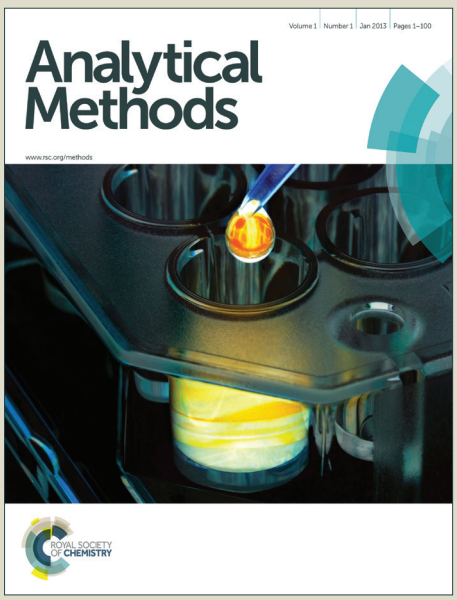

This is an *Accepted Manuscript*, which has been through the Royal Society of Chemistry peer review process and has been accepted for publication.

Accepted Manuscripts are published online shortly after acceptance, before technical editing, formatting and proof reading. Using this free service, authors can make their results available to the community, in citable form, before we publish the edited article. We will replace this *Accepted Manuscript* with the edited and formatted *Advance Article* as soon as it is available.

You can find more information about *Accepted Manuscripts* in the Information for Authors.

Please note that technical editing may introduce minor changes to the text and/or graphics, which may alter content. The journal's standard Terms & Conditions and the Ethical guidelines still apply. In no event shall the Royal Society of Chemistry be held responsible for any errors or omissions in this *Accepted Manuscript* or any consequences arising from the use of any information it contains.

ROYAL SOCIETY OF CHEMISTRY

www.rsc.org/methods

Cite this: DOI: 10.1039/c0xx00000x

www.rsc.org/xxxxxx

ARTICLE TYPE

Handheld and non destructive methodologies for the compositional investigation of meteorite fragments

Vincenza Crupi,*[a] Alessandra Giunta,[b] Barry Kellett[b], Francesca Longo,[a] Giacomo Maisano,[a] Domenico Majolino,[a] Antonella Scherillo[c] and Valentina Venuti[a]

Received (in XXX, XXX) Xth XXXXXXXXX 20XX, Accepted Xth XXXXXXXXX 20XX
DOI: 10.1039/b000000x

In the present study, an innovative methodological approach has been proposed in order to characterize meteoritic samples without removing or causing damage to any part of them. In particular, Raman and X-ray fluorescence (XRF) measurements have been preliminarily performed, using portable instruments, in order to obtain qualitative and semi-quantitative compositional information, respectively. These analyses have been followed and supported by time of flight neutron diffraction (TOF-ND) experiments, which allowed us to perform quantitative mineralogical phase analysis. Such a methodological approach was tested on four meteoritic samples, of different type and size, coming from several different regions of the Solar System (e.g., the Moon, Mars and asteroids). The validity and strength of the results obtained using these techniques are discussed and compared with results available in literature.

1 Introduction

Meteorites are of fundamental importance for the study of our Solar System,[1-3] as they are witness to early planet accretion and evolution processes. Their uniqueness lies in the fact that, having wandered through interplanetary space for billions of years, they did not suffer recent changes in chemical and physical properties, and hence remained geologically frozen in time. This gives them a key role: that of "snapshots" of ancient times. Through their study it is then possible to trace the history and evolution that gave rise to our own planet Earth, helping us better understand our own origins and conditions for the onset and proliferation of life.

These are the main reasons that make the meteorites a topic of great interest and fundamental importance, involving interdisciplinary areas of research, ranging from astrophysics and nuclear physics to chemistry and mineralogy.

Until not long ago, study of meteorite bulk characteristics were performed by using destructive or semi-destructive analytical techniques. These include a wide range of chemical dissolution methods (such as inductively coupled plasma atomic emission and mass spectroscopy, i.e. ICP-AES and ICP-MS), methods that require sample irradiation (instrumental neutron activation analysis, i.e. INAA) or powdering of material (x-ray fluorescence and diffraction, i.e. XRF and XRD), or methods requiring preparation of a thin or thick section (such as electron scanning microscopy, i.e. SEM, or Raman spectroscopy). However, due to the high economic and scientific value of these samples, it is clear that it is appropriate to preserve their integrity as much as possible. This entails the need to implement analytical techniques which do not damage in any way the meteorites under study.

The present paper is aimed at determining a methodological approach of analytical techniques for the compositional and mineralogical characterization, at elemental and microscopic length scale, of a meteoritic sample in a non-invasive way (i.e., without sample preparation or destruction).

We have employed both X-ray fluorescence (XRF) and Raman spectroscopy using portable equipments. Furthermore, time of flight neutron diffraction (TOF-ND) measurements have been performed on the INES beamline, operating at the spallation source ISIS, UK. These methodologies are widely used in the study of the structure of matter,[4-7] but not yet widespread in the analysis of meteorites. Their implementation for the analysis of meteorites is, therefore, the purpose of this work, as well as the results achieved about the composition.

The semi-quantitative elemental and mineralogical studies, using XRF and Raman techniques respectively, offered the advantage of the short time needed for the measurement and the possibility of performing *in situ* investigation. The use of TOF-ND, in addition to the quantification of the mineralogical phases, allowed the discrimination of minerals which belong to the same mineralogical group and can exhibit the same vibrational modes. These are not distinguishable using Raman technique only.

Thus, the joint use of XRF, Raman and TOF-ND provides a comprehensive approach to this kind of analysis to characterise the chemical composition and mineralogical makeup of different meteorite samples.

Such procedure has been tested on four meteoritic samples of different type and dimension, coming from different parts of the Universe. Its validity is demonstrated by comparing the obtained results with the information gathered from literature.

2 Materials

Mars meteorite: Sayhal Uhaymir 008.

Analytical Methods Accepted Manuscript

The meteorite Sayhal Unaymir 008 (SaU 008),[8-12] also known as martian basalt, is a an achondritic meteorite belonging to the shergottite class. It was found in the Asian state of Oman on 26th of November 1999. Five greenish-gray fragments that are macroscopically identical were found in two places at a distance of approximately 1864 m. In particular, SaU 005 indicates a fragment of 547 g and two fragments of 561 g and 236 g, which are partially covered by fusion crust and show regmaglites; whereas SaU 008 specifies a rather large fragment of 7805 g and a smaller one of 774 g. On the latter, the black fusion crust is almost completely preserved. The total mass of SaU 005/008 is 9923 g.

Fig. 1 shows the fragment of SaU 008 which has been investigated for this work. Its weight is 0.26 g. The sample was purchased from a reputable dealer.

Fig. 1 Photo of the investigated SaU 008 chip.

The identified mineral phases are maskelynite, olivine (forsterite) and pyroxene (augite and pigeonite).[8-12] From the petrographic point of view, the meteorite presents a porphyritic texture with phenocrysts of olivine immersed in the bulk, with a strong glassy component, which primarily consists of pigeonite and maskelinite.

Carbonaceous chondrite: Allende.

The Allende meteorite[10,13,14] was found in Mexico in 1969, at the village of Pueblito Allende, the fragments of the meteorite fallen from the sky were distributed over an area of 50 km^2. This meteorite belongs to the class of the carbonaceous chondrites of CV3 type, and may, therefore, contain a relatively high percentage of carbon (C) (up to 6%). It is formed of primitive Solar System accreationary materials that have been dated to about 4.56 billion years.

For this study, two samples of the Allende meteorite have been analysed: a larger chip, weighing 2.83 g, and a smaller chip, weighing 0.44 g. In Fig. 2 the investigated samples of the Allende meteorite are shown.

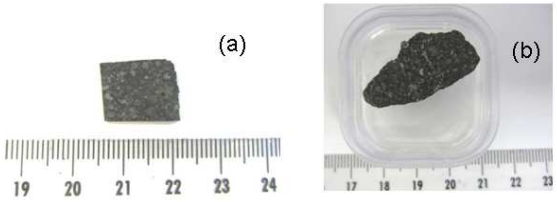

Fig. 2 Photos of the investigated Allende (a) small and (b) large chips.

From a mineralogical point of view, the Allende, as a carbonaceous chondrite, is reported to contain chlorite, davisite, feldspar (mainly calcium), gypsum, graphite, olivine (forsterite and fayalite), panguite, pyroxene (augite, bronzite, enstatite and pigeonite), serpentine (antigorite and lizardite) and finally spinel (especially chromite).

Studies carried out on fragments of Allende meteorite[10,13,14] revealed three distinct components: a black fine-grained matrix, chondrules and white irregular aggregates. The matrix is mainly composed of olivine rich in iron, with minor amounts of troilite, pentlandite and taenite, made opaque by the diffusion of carbonaceous material. Most of the chondrules are revealed to be rich in magnesium and to consist of olivine with minor amounts of clinoenstatite and glassy material. Few chondrules of this meteorite are rich in calcium and aluminum, and largely consist of anorthite, gehlenite, augite, and spinel. Finally, the irregular white coloured aggregates are rich in calcium and aluminum and for this indicated as CAIs (calcium aluminum rich inclusions), and may contain anorthite, gehlenite, augite, spinel, nepheline, grossular and sodalite.

Lunar highlands sample: Dar Al Gani 400.

The Dar al Gani 400 (DaG 400) meteorite originates from the Moon and is an achondrite. The sample is a feldspathic regolith breccia and is believed to originate from the lunar highlands. For our measurements, we used a small fragment weighing around 0.44 g (Fig. 3). As illustrated in the figure, on the bulk, the sample consists of a dark impact melt rich matrix, with white grains that are anorthositic feldspar rich.

Fig. 3 Photo of the investigated DaG 400 chip.

Previously studies[2] of DaG 400 revealed that the sample has a bulk composition typical of the lunar highlands, with high Al and Ca, relative to Mg and Fe. The meteorite is reported[15-19] to be composed of mainly feldspathic glass with anorthite, olivine, pyroxene, and minor amounts of ilmenite. Among the accessory phases it may include silica, calcite (which is terrestrial rather than lunar in origin), troilite, FeNi metal and spinel (such as chromite). Some studies have indicated fayalite and forsterite as types of olivine, and various pyroxenes, such as augite, diopside, enstatite, ferrosilite and pigeonite have been identified.

Analytical Methods Accepted Manuscript

Ordinary chondrite: Northwest Africa 869.

The NWA 869 meteorite is an ordinary chondrite found in North-Western Africa in 2000. The sample under investigation (Fig. 4) weighs 2.56 g, and, from its visual analysis, chondrules are fairly evident on its surface.

Fig. 4. Photo of the investigated NWA 869 chip.

Previous studies on this meteorite[8,9,20-22] have identified its chemical and mineralogical composition. The main mineral phases present are feldspar (mainly calcium), olivine (forsterite and fayalite), pyroxene (ferrosilite and pigeonite) spinel and FeNi metal. Raman measurements carried out on a fragment of NWA 869 indicated the presence of pigeonite, olivine and feldspar (probably orthoclase.

In Table 1 we listed all the investigated samples, indicating their provenance and classification.

Table 1 List of investigated meteorites, together with some information, such as the official abbreviation, the indication of the place and date of fall or discovery and their classification. There is no official abbreviation for Allende.

Sample	Abbreviation	The place of fall or discovery	Date of fall or discovery	Classification
Sayh al Uhaymir 008	SaU 008	Oman	1999	Martian (basaltic shergottite)
Allende	-	Mexico	1969	Carbonaceous chondrite
Dar al Gani 400	DaG 400	Libya	1998	Lunar (anorth)
Northwest Africa 869	NWA 869	Northwest Africa	2000	Ordinary chondrite

3 Methods

XRF measurements

XRF measurements were performed using the portable XRF analyzer "Alpha 4000" (Innov-X System), equipped with an X-ray tube with Ta anode, a high resolution Si PIN diode detector (FWHM < 220 eV at 5.95 keV for Mn k_α line) and a 2 mm aluminium filter. The spot size for this analyzer is approximately 170 mm^2. Control of the instrument and data storage was performed through a Hewlett Packard iPAQ Pocket PC. The instrument operated in "Soil" mode and two sequential tests were performed on each sample. The operating conditions were 40 kV and 7 μA for the first run, and 15 kV and 5 μA for the second one. In the first case, we have been able to detect elements from P to Pb. In the second case, by using the program LEAP (Light Element Analysis Program), the elements from P to Fe have been detected with higher accuracy than the first run. The calibration was performed by the standard Innov-X systems in-house procedure (Soil LEAP II), and was verified using alloy certified reference materials produced by Analytical Reference Materials International. In addition, the accuracy of portable XRF measurements was also successfully checked by analyzing a group of international rocks standards including: AL-1 (Albite), BR (Basalt), BCR-1 (Basalt), BHVO-1 (Basalt), BIR-1 (Basalt), DNC-1 (Dolerite), DR-N (Diorite), DT-N (Kyanit), GA (Granite), GS-N (Granite), GSP-1 (Granodiorite), KK (Bauxite), NIM-G (Granite), NIM-N (Norite), SCO-1 (Mudrock), SDC-1 (Micashist), SGR-1 (Mudrock), and W-2 (Diabase). The results were compared with the certified values, and the resulting correlation coefficients for the selected elements was ≈0.98. Measurements have been performed directly on the surface of each meteoritic fragment, without any specific preparation of the sample. Three sets of measurements for each sample have been performed, and for each test the acquisition time was 60 s.[23]

Raman measurements

Raman measurements were carried out by the portable "BTR111 MiniRam^{TM}" (BW&TEK Inc) spectrometer using an excitation wavelength of 785 nm (diode laser), ~ 280 mW laser power and CCD detector (TE cooled). The system was equipped with a fiber optic interface for convenient sampling. The spectra were performed in the wavenumber range from 60 to 3150 cm^{-1}. For each Raman measurement the acquisition time was 40 s and several scans have been accumulated for each spectrum to improve the signal-to-noise ratio. The experimental spectra were compared with those from various database.[24-26]

TOF-ND measurements

A detailed description of the TOF neutron diffraction (TOF-ND) technique, together with the fundamental advantages of its use in a variety of fields included the study of meteorites, has been already reported in literature[27]. Here, we recall the key features.

In a TOF neutron diffraction experiment the scanning is performed at fixed angles using a non-monochromatic beam containing several wavelength of the incident neutrons[28]. A schematic representation is reported in Fig. 5 (left panel). The material composition and crystal structure can be derived by determining the symmetry characteristics of the sample given by the distribution of Bragg peaks as a function of crystallographic planes (d-spacing). In particular, by using the de Broglie relationship, the energy dispersion is obtained by measuring the time-of-flight t that a neutron takes to cover the distance L ($L = L_1+L_2$ in Fig. 5.) from the source to the detector. Under the assumption that the neutrons do not suffer a change in energy during the scattering process, the time-of-flight values are directly related to the distance d between the crystallographic planes by:

$$d = \frac{h}{2m_n}\frac{t}{L\sin\vartheta} \qquad (1)$$

where 2ϑ is the scattering angle, h the Planck constant and m_n the neutron mass. This is the fundamental equation of TOF

Analytical Methods Accepted Manuscript

diffraction. The efficiency of TOF diffractometers is increased by using many detector tubes aligned in detector banks, so reducing the data collection time and focusing the superposing spectra afterwards.

The measured neutron diffraction pattern is available for quantitative phase analysis by assuming that each phase exhibits a unique set of diffraction peaks, whose intensity is proportional to the phase content in the mixture, and that the total diffraction pattern will contain the weighted sum of the single phase contributions.

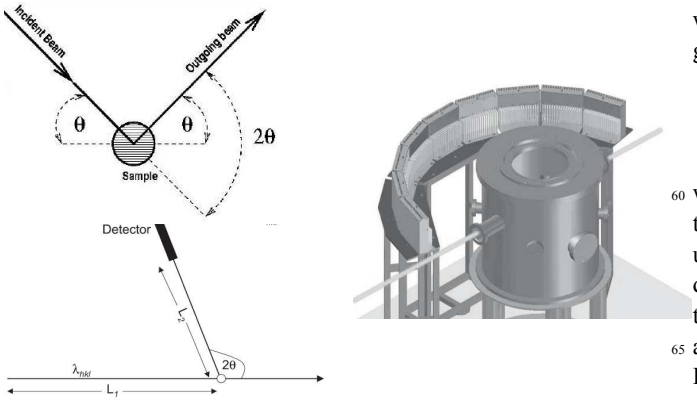

Fig. 5. On the left: basic principle of a TOF-ND experiment, the total flight $L = L_1 + L_2$. On the right: INES layout showing the sample chamber (the primary neutron beam goes from left to right) and the nine detector banks.

The experiments were performed at the TOF diffractometer INES, installed at the ISIS spallation source at the Rutherford Appleton Laboratory (UK). The instrument layout is shown in the right panel of Fig. 5. The diffractometer is equipped with 144 squashed ^{3}He detectors covering 2ϑ angles from 19.2° to 163.2° in the horizontal scattering plane. The detectors are grouped into 9 banks, each bank being composed of 16 detectors that lie on a circle of 1 m radius from the diffractometer centre. The wide angular range covered by the detectors, together with the thermal neutron beam coming from the water moderator (incident wavelength range extending from 0.17 Å to 3.24 Å) allows the investigation of a *d*-spacing range from ~ 0.4 Å to ~ 16 Å and high resolution up to $\Delta d/d$ = ~ 0.1% in backscattering.

Static measurement configurations and relatively long acquisition times (6–7 h) were used for measurements on large meteoritic fragments without any prior preparation. The activation induced by the measuring procedure was negligible and disappeared within a few minutes/hours. The sample container is a large vacuum tank (80 cm diameter and about 0.5 m^3 volume). Each object has been studied with a single sampling by using a beam size of 30 × 30 mm^2. In most cases the beam area covered the whole meteorite fragment examined, thus allowing a reliable determination of the average composition. The nine detector banks on INES provide nine diffraction patterns covering different *d*-spacing ranges with different resolution. According to Eq. (1), the smaller the detector angle, the longer the accessible *d*-spacing. Backscattering (high-angle) detectors provide the small *d*-spacing range in high resolution, whereas forward scattering (small angle) detectors provide a wider *d*-spacing range in lower resolution. The low-*d* region is the area with the highest density of peaks, whereas in the high-*d* region only few peaks are present that are, nevertheless, the most important for the identification of the phases.

The data have been normalized to the number of counts (through the incident monitor) and divided by a vanadium rod spectrum in order to account for the detectors' efficiency.

The data treatment followed the well-established quantitative Rietveld analysis for phase identification and quantitative assessment of the material's composition, using the public-domain program suite GSAS[29] with the graphical interface EXPGUI.[30] This procedure is based on the assumption that the weight fraction W_i of the i-th phase in a multiphase mixture is given by the normalized product

$$W_i = \frac{S_i Z_i M_i V_i}{\sum_n S_n Z_n M_n V_n}, \qquad (2)$$

where S, Z, M and V are the refined Rietveld scale factor, the number of formula units per unit cell, the mass of the formula unit and the unit cell volume, respectively. The sum in the denominator accounts for all the crystalline phases revealed by the experimental diffraction pattern. The fitting procedure used is a least-squares minimization. For all the minerals one common Debye–Waller factor (which describes the attenuation of coherent neutron scattering caused by thermal motion) has been used. For each phase, the corresponding structural parameters were obtained from the Inorganic Crystal Structure Database (ICSD).

Realistic estimates of the uncertainties on the weight fraction values are about 0.5% for all investigated samples. This means that all those mineral phases whose weight fraction is below this value have to be considered as not present. We remark that the Rietveld analysis has been performed on the nine simultaneously collected data sets from the nine independent detector groups with phase fractions as free parameters.

4 Results and discussion

First of all, portable XRF and Raman measurements were applied in order to achieve the semi-quantitative chemical composition and mineralogical makeup of all samples.

In particular, as far as XRF data are concerned, it is worth remarking that since they have been collected directly on the sample surface without any specific preparation, what is obtained is only semi-quantitative surface elemental composition. Even though the penetration depth of an X-ray source is of the order of few microns, the XRF spectra will reflect the composition of the surface of the whole sample (including the meteorite and any terrestrially deposited phases during residence on the Earth's surface), together with some bulk contribution. The XRF results are reported in Table 2, the grouping of the detected elements in *major*, *minor* and *trace* was obtained by comparing the corresponding peaks area as calculated through the standard routine of the Innov-X software that takes into accont also the sensitivity of the instrument for each detected element.

Raman analysis was performed in order to test the reliability of a portable instrumentation on the mineralogical characterization of meteorites. The XRF and Raman results are summarized in Tables 2 and 3, respectively.

Table 2 Elements detected by XRF analysis.

Analytical Methods Accepted Manuscript

Sample	Major elements	Minor elements	Elements in trace
SaU 008	Ca, Fe	Cr, K, Mn, Ti	Ba, Mo, Pb, Sr, Zn, Zr
Allende	Ca, Fe, S	Cr, K, Mn, Ni, Ti	Mo, Sr, Pb, Zn, Zr
DaG 400	Ca, Fe	Cr, K, Mn, Sr, Ti	Mo, Ni, Zr
NWA 869	Ca, Fe, S	Cr, K, Mn, Ni, Ti	Au, Mo, Pb, Rb, Sr, Zn, Zr

Table 3 Minerals identified obtained by Raman spectra.

Sample	Minerals
SaU 008	Pyroxene
Allende	Olivine, graphite
DaG 400	Plagioclase, calcite
NWA 869	Olivine

Then, the use of TOF-ND allowed us to obtain, in a non-destructive way, a quantitative characterization of mineral phase fractions. The results are reported in Table 4 for all the investigated samples. All the mineral weight fractions have been normalized to one.

Table 4 Phase quantification from TOF-ND data. Pigeonite: Pi, augite: Au, forsterite: Fo, anorthite: An, orthoclase: Or, chromite: Ch, ulvospinel: Ul, graphite: Gr, spinel: Sp, troilite: Tr, tetrataenite: Te, nepheline: Ne, enstatite: En, ferrosilite: Fer, fayalite: Fa, iron: Fe, taenite: Ta, schreibersite: Sc.

SaU 008						
Pi	**Au**	**Fo**	**An**	**Or**	**Ch**	**Ul**
0.352	0.141	0.323	0.007	0.031	0.037	0.109

Allende								
Fo	**Gr**	**Pi**	**Sp**	**Tr**	**Au**	**Te**	**An**	**Ne**
0.585	0.009	0.031	0.074	0.041	0.098	0.024	0.124	0.014

DaG 400							
An	**Fo**	**Au**	**En**	**Fer**	**Pi**	**Ch**	**Sp**
0.476	0.146	0.025	0.026	0.018	0.297	0.003	0.009

NWA 869							
Fa	**Pi**	**Fo**	**Fer**	**Or**	**Fe**	**Ta**	**Sc**
0.012	0.043	0.851	0.030	0.053	0.004	0.004	0.003

The consistency of the data obtained by the different techniques and their agreement with literature data will be discussed and used as key-parameter for testing, for each sample, the validity of this multi-methodological approach.

Sayhal Uhaymir 008

Fig. 6 reports the typical XRF spectra collected in the two sequential tests for SaU 008 sample. The analysis of the three sets of XRF measurements revealed a substantial consistency of the various results (see Table 2).

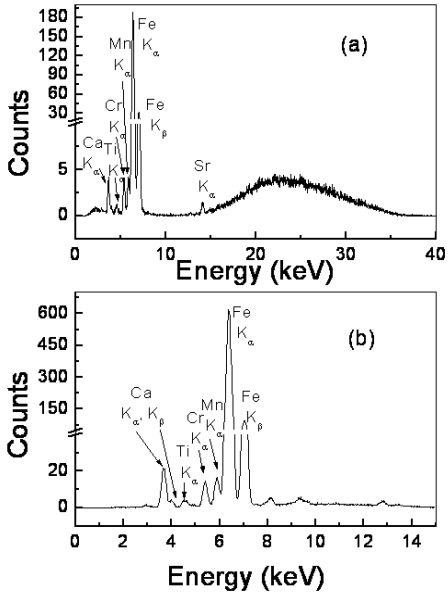

Fig. 6 XRF spectra of SaU 008 measured with the X-ray tube operating at 40 kV (a) and 15 kV (b).

The analysis of Raman spectra allowed us to detect only the presence of pyroxene (see Table 3). This result is in agreement with literature.[10-12] Furthermore, the chemical composition of the identified mineral is consistent with our XRF data.

The weight fractions of the mineralogical phases, as obtained by TOF-ND, are reported in Table 4. The total phase fraction coming from pyroxenes, recognized as pigeonite and augite, turns out to be ~ 50%. This fulfils the Raman qualitative information of pyroxene as being an observed phase. Furthermore, the detected presence of pigeonite (~ 35%) and ulvöspinel (~ 11%), Fe- and Ca- rich minerals, is in agreement with XRF results, which indicated Fe and Ca as major chemical elements.

Allende

In the case of Allende sample, the XRF analysis performed on different parts of the sample revealed a relative abundance of calcium (Ca) and iron (Fe) (see Table 2), in agreement with literature data.[10,13,14]

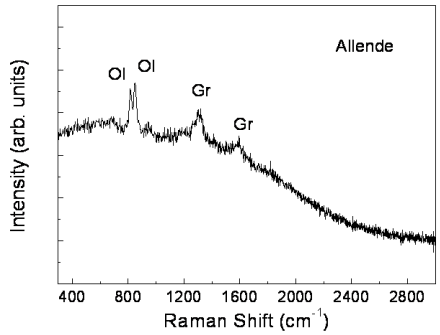

Fig. 7 Raman spectrum of Allende sample. Ol: Olivine; Gr: Graphite.

Analytical Methods Accepted Manuscript

Fig. 7 shows the Raman spectrum collected for the large Allende fragment. The obtained Raman results (see Table 3) appear in agreement with literature reported minerals[10,13,14] and with the chemical composition as obtained from the XRF analysis. The characteristic peaks of olivine ($(Mg,Fe)_2SiO_4$) in the 800 ÷ 900 cm^{-1} region, produced by the symmetric stretching vibration of SiO_4 group, are well evident. Again, two bands associated to graphite are clearly distinguishable. In particular, the band at ~ 1580 cm^{-1} is usually referred to as the G-band, and the other band at ~ 1300 cm^{-1} is denoted as disorder band (D-band).[31]

The presence of graphite is justified by the definition of carbonaceous chondrites as having a relatively high percentage of carbon (up to 6%) in a form of graphite called cliftonite. Its existence, being this mineral constituted of only carbon, cannot be detected by XRF.

The measured neutron diffraction patterns for Allende are depicted in Fig. 8 (crosses), together with the best fit of the data (solid lines) and residuals (bottom curves). The three detector banks which have been selected represent backscattering ((a), (b) cases) and forward ((c) case) configurations, centred at (a) 2ϑ ~ 127.2°, (b) 2ϑ ~ 91.2°, and (c) 2ϑ ~ 55.2°. The corresponding phase quantification is reported in Table 4.

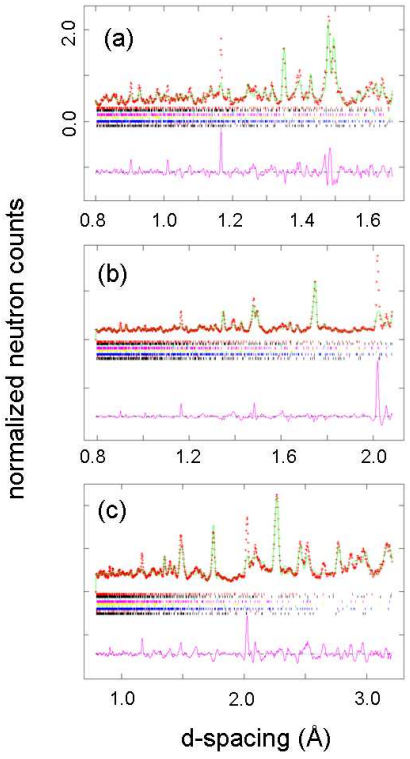

Fig. 8 TOF backscattering (a), (b) and forward (c) neutron diffraction pattern for the meteorite Allende. The theoretical peak position of the different mineralogical phases included in the model is indicated by the bars at the bottom of the pictures. From bottom to top: Fo, Gr, Pi, Sp, Tr, Au, Te, An, Ne.

The main mineralogical phase is olivine, represented by forsterite (~ 58%). This confirms the presence of olivine as qualitatively estimated by Raman technique (see Table 3). Traces of graphite are also observed, supporting the aforementioned interpretation of the Raman bands. Furthermore, the observation, by XRF, of sulphur as major element is well compatible with the revealed presence of troilite (FeS), whereas Ca and Fe are recognized in almost all the other identified mineralogical phases.

Dar Al Gani 400.

From the study of the XRF spectra (see in Fig. 9) obtained for the fragment Dar Al Gani 400 (DaG 400), it was observed (see Table 2) the presence, as major elements, of Ca and Fe, fully compatible with the chemical and mineralogical composition of lunar samples.

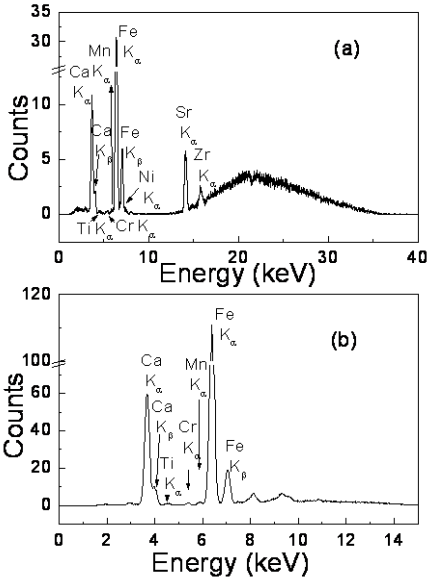

Fig. 9 XRF spectra of DaG 400 measured with the X-ray tube operating at 40 kV (a) and 15 kV (b).

Raman measurement, performed on a white grain of the sample, is displayed in Fig. 10.

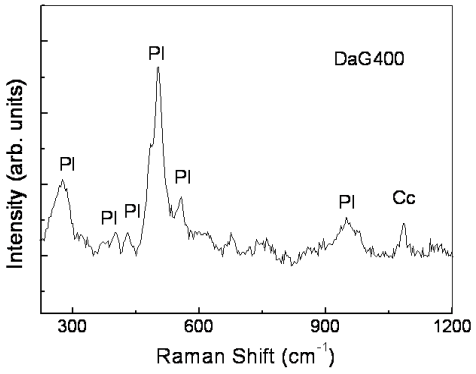

Fig. 10 Raman spectrum of DaG 400 sample. Pl: Plagioclase; Cc: calcite.

The mineralogical phases obtained from Raman technique are

Analytical Methods Accepted Manuscript

shown in Table 3. Almost all the observed Raman bands can be associated to a calcic plagioclase, a typical feldspar found in lunar rocks and identified as a solid solution of anorthite $CaAl_2Si_2O_8$ and albite $NaAlSi_3O_8$.[32] A contribution associated to calcite is also evident in the Raman spectrum, that can be due to the terrestrial weathering of this sample. The obtained results are in almost good agreement with literature.[3,15-19]

The comparison between the Raman and XRF data shows that the observed mineral phases are in clear agreement with the chemical elements detected for the sample. Calcite ($CaCO_3$) and calcic plagioclase are both Ca-rich minerals and Ca was identified as a major element for this meteorite.

As far as TOF-ND results are concerned, by looking at the phase quantification in Table 4, we can observe, for this sample, anorthite as main mineralogical phase (~ 48%), confirming Raman results and in agreement with the literature data. Again, almost all the observed mineralogical phases contain Ca and Fe, confirming the elemental composition by XRF.

NWA-869

The chemical species characterizing the NWA 869 sample are reported in Table 2. There is good consistency between literature data and for that resulting from our study,[20-22] with the only differences related to the trace elements, which is an indication of the reliability of the handheld XRF technique as a tool for preliminary semi-quantitative analysis.

The Raman analysis (see Table 3) of the sample NWA 869 allowed us to identify as mineral phase only olivine. This result is, again, in agreement with the information provided by literature.[20-22] Since in chondrites olivine is known to be mid-Fo composition, by only looking at the Raman spectra we are not confident in hypothesizing fayalite (Fe_2SiO_4) as the main olivine component, and in this sense the analysis of TOF-ND data will be crucial in clarifying the nature of the observed phase. This could be in contrast with the observation, by XRF, of iron as major element, but, on the other side, Fe can be justified as metal or due to suphide phases.

The measured neutron diffraction patterns for NWA 869 are displayed in Fig. 11 (crosses), together with the best fit of the data (solid lines) and residuals (bottom curves). As for the Allende sample, backscattering (a, b) and forward (c) configurations, centred at (a) $2\vartheta \sim 127.2°$, (b) $2\vartheta \sim 91.2°$, and (c) $2\vartheta \sim 55.2°$, are reported.

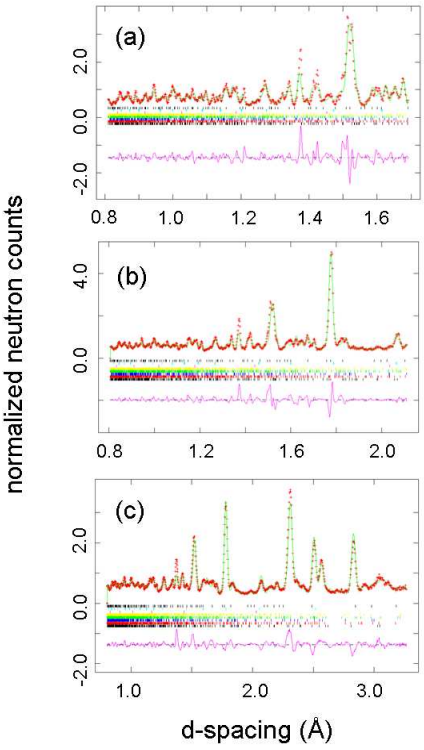

Fig. 11 TOF backscattering (a), (b) and forward (c) neutron diffraction pattern for sample NWA 869. The theoretical peak position of the different mineralogical phases included in the model is indicated by the bars at the bottom of the pictures. From bottom to top: Fa, Pi, Fo, Fer, Or, Fe, Ta, Sc.

From Table 4 it is evident that the major phases are represented by olivine (as forsterite, ~ 85%), in agreement with Raman results. The apparent disagreement with the observation, by XRF, of sulphur, and the composition by TOF-ND, which did not reveal any mineralogical phase containing S, can be overcome taking into account that, as reported in literature for ordinary chondrites, sulphides are typically found outside of chondrules as isolated grains.[21] Then, on one side, they cannot be detected by neutrons, which access only to the bulk composition.[27] On the other side, as reported in literature,[21] the bulk chemical compositions of NWA 869 obtained by XRF analysis did not show the presence of S.

Conclusions

In the present paper, a non destructive approach for the compositional and mineralogical analysis of meteoritic samples, based on a combination of XRF, Raman, using portable instruments, and TOF-ND measurements, at the Large Facilities has been for the first time tested and validated on a martian (SaU 008), a lunar (DaG 400) and two asteroidal meteorites (Allende, NWA 869). The correspondence of the data extracted from the different techniques has been checked, together with their agreement with the information reported in literature.

Taking into account the versatility of the employed techniques together with, at the same time, the remarkable results that can be achieved, we propose that this methodological approach represents a key-step for the evolution of the study of meteorites.

Analytical Methods Accepted Manuscript

Finally, the described analysis by XRF and Raman portable equipments opens the way for the direct exploration of extraterrestrial spaces, and hence can be profitably used to make measurements directly on those interplanetary sites of scientific interest.

Acknowledgements

The authors are grateful to Katherine Joy of University of Manchester, School of Earth Atmosphere & Environmental Science (England) for providing the Allende and NWA 869 samples.

Notes and references

[a] *Dipartimento di Fisica e di Scienze della Terra, Università degli Studi di Messina, Viale Ferdinando Stagno D'Alcontres 31, 98166, Messina, Italy. Fax:+39 090 395004; Tel:+39 090 6765447; E-mail: vcrupi@unime.it*

[b] *STFC RAL Space, Rutherford Appleton Laboratory, Chilton, Didcot, Oxon. OX11 0QX, UK.*

[c] *STFC RAL ISIS, Rutherford Appleton Laboratory, Chilton, Didcot, Oxon. OX11 0QX, UK.*

1 Z. Ceplecha, J. Borovicka, J. G. Elford, D. O. Revelle, R. L. Hawkes, V. Porubcan and M. Šimek, Meteor phenomena and bodies, *Space Sci. Rev.*, 1998, **84**, 327-471.

2 D. S. McKay, E. K. Gibson, Jr. K. L. Thomas-Keprta, H. Vali, C. S. Romanek, S. J. Clemett, X. D. F. Chillier, C. R. Maechling and R. N. Zare, Search for past life on Mars: possible relic biogenic activity in martian meteorite ALH84001, *Science*, 1996, **273**, 924-930.

3 K. H. Joy, I. A. Crawford, S. S. Russell and A. T. Kearsley, Lunar meteorite regolith breccias: an in situ study of impact melt composition using LA-ICP-MS with implications for the composition of the lunar crust, *Meteorit. Planet. Sci.*, 2010, **45**, 917-946.

4 G. Barbera, G. Barone, V. Crupi, F. Longo, D. Majolino, P. Mazzoleni and V. Venuti, Nondestructive analyses of carbonate rocks: applications and potentiality for museum materials, *X-Ray Spectrom.*, 2013, **42**, 8-15.

5 G. Barone, V. Crupi, F. Longo, D. Majolino, P. Mazzoleni, S. Raneri and V. Venuti, A multi-technique approach for the characterization of decorative stones and non-destructive method for the discrimination of similar rocks, *X-Ray Spectrom.*, 2013, DOI: 10.1002/xrs.2520.

6 G. Barone, L. Bartoli, C. M. Belfiore, V. Crupi, F. Longo, D. Majolino, P. Mazzoleni and V. Venuti, Comparison between TOF-ND and XRD quantitative phase analysis of ancient potteries *J. Anal. At. Spectrom.*, 2011, **26**, 1060-1067.

7 R. Bellissent, G. Galli, T. Hyeon, S. Magazù, D. Majolino, P. Migliardo, K. S. Suslick, Structural properties of amorphous bulk Fe, Co, and Fe-Co binary alloys, *Physica Scripta*, 1995, **T57**, 79-83.

8 M. Fornaseri, *Lezioni di Geochimica*, Vestri, Roma, 1974.

9 G. Ottonello, *Principi di Geochimica*, Zanichelli, Bologna, 1991.

10 http://www.lpi.usra.edu/meteor/metbull.php (Meteoritical Bullettin Database)

11 J. N. Grossman, The Meteoritical Bullettin, No. 84, 2000 August, *Meteorit. Planet. Sci.*, 2000, **35**, A199–A225.

12 Y. Yu and J. S. Gee, Spinel in martian meteorite SaU 008: implications for martian magnetism, *Earth Planet. Sci. Lett.*, 2005, **232**, 287 – 294.

13 http://hdl.handle.net/10088/809.

14 Meteoritical Bulletin no. 45, Moscow, 1969, reprinted Met. **5**, 1970, 85-109.

15 A. S. Semenova, M. A. Nazarov, N. N. Kononkova, A. Patchen and L. A. Taylor, Mineral chemistry of lunar meteorite Dar Al Gani 400 (Abstract), *Lunar Planet. Sci. Conf.*, 2000, **31**, 1252.

16 B. A. Cohen, T. D. Swindle and D. A. Kring, Geochemistry and ^{40}Ar-^{39}Ar geochronology of impact-melt clasts in feldspathic lunar meteorites: implications for lunar bombardment history, *Meteorit. Planet. Sci.*, 2005, **40**, 755–777.

17 K. H. Joy, I. A. Crawford, S. S. Russell, B. Swinyard, B. Kellett and M. Grande, Lunar regolith breccias MET 01210, PCA 02007 and DAG 400: their importance in understanding the lunar surface and implications for the scientific analysis of D-CIXS data, *Lunar Planet. Sci. Conf.*, 2006, **37**, 1274.

18 M. Bukovanska, G. Dobosi, F. Brandstätter and G. Kurat, DAR AL GANI 400: petrology and geochemistry of some major lithologies, *Meteorit. Planet. Sci.*, 1999, **34**, Supplement, A21.

19 R. L. Korotev, Lunar geochemistry as told by lunar meteorites, *Chemie der Erde*, 2005, **65**, 297–346.

20 H. C. Connolly, J. Zipfel, J. N. Grossman, L. Folco, C. Smith, R. H. Jones, K. Righter, M. Zolensky, S. S. Russell, G. K. Benedix, A. Yamaguchi and B. A. Cohen, The Meteoritical Bulletin, No. 90, 2006 September, *Meteorit. Planet. Sci.*, 2006, **41**, 1383-1418.

21 K. Metzler, The L3–6 chondritic regolith breccia Northwest Africa (NWA) 869: (I) Petrology, chemistry, oxygen isotopes, and Ar-Ar age determinations, *Meteorit. Planet. Sci.*, 2011, **46**, 652–680.

22 K. Metzler, A. Bischoff, H. Palme and M. Gellissen, Impact melt rocks from the L3-6 chondritic regolith breccia Northwest Africa (NWA) 869 (Abstract), 73th Annual Meteoritical Society Meeting, 2010, New York, *Meteorit. Planet. Sci.*, 2010, **45**, A137.

23 https://innovx.ca/.

24 RRUFF Project, 2010, Department of Geosciences, University of Arizona, Tucson, USA. http://rruff.info/. Accessed 08 apr 2013.

25 Handbook of Raman spectra http://ens-lyon.fr/LST/Raman.

26 A. I. Apopei, N. Buzgar, A. Buzatu, Raman Data Search and Storage (RDSS): A Raman spectra library software using peak positions for fast and accurate identification of unknown inorganic compounds, 2013, http://rdrs.uaic.ro/. Accessed 08 apr 2013.

27 W. Kockelmann, A. Kirfel and E. Haehnel, Non-destructive phase analysis of archaeological ceramics using TOF neutron diffraction, *J. Arch. Sci.*, 2001, **28**, 213-222.

28 B. T. M. Willis, Crystallography with a pulsed neutron source, *Z. Kristallogr.*, 1994, 209, 385–391.

29 A. C. Larson, R. B. Von Dreele, 2004, GSAS: general structure analysis system, Los Alamos Laboratory Report LAUR No. 86-748 Los Alamos, NM, USA.

30 B. H. Toby, EXPGUI, a graphical user interface for GSAS, *J. Appl. Crystallogr.*, 2001, **34**, 210–213.

31 K. L. Larsen and O. F. Nielsen, Micro-Raman spectroscopic investigations of graphite in the carbonaceous meteorites Allende, Axtell and Murchison, *J. Raman Spectrosc.,* 2006, **37**, 217-222.

32 A. Wang, B. L. Jolliff and L. A. Haskin, Raman spectroscopy as a method for mineral identification of lunar robotic exploration missions, *J. Geophys. Res.*, 1995, **100**, 189-199.

Analytical Methods Accepted Manuscript